BIOCHEMISTRY
including biophysical chemistry & molecular biology
Article

Biochemistry **2009,** *48,* 9405–9415 9405
DOI: 10.1021/bi900959c

A Potentially Versatile Nucleotide Hydrolysis Activity of Group II Chaperonin Monomers from *Thermoplasma acidophilum*†

Kentaro Noi, Hidenori Hirai, Kunihiro Hongo, Tomohiro Mizobata, and Yasushi Kawata*

Department of Chemistry and Biotechnology, Graduate School of Engineering, and Department of Biomedical Science, Institute of Regenerative Medicine Biofunction, Graduate School of Medical Science, Tottori University, Tottori 680-8552, Japan

Received June 7, 2009; Revised Manuscript Received September 2, 2009

ABSTRACT: Compared to the group I chaperonins such as *Escherichia coli* GroEL, which facilitate protein folding, many aspects of the functional mechanism of archaeal group II chaperonins are still unclear. Here, we show that monomeric forms of archaeal group II chaperonin α and *β* from *Thermoplasma acidophilum* may be purified stably and that these monomers display a strong AMPase activity in the presence of divalent ions, especially Co^{2+} ion, in addition to ATPase and ADPase activities. Furthermore, other nucleoside phosphates (guanosine, cytidine, uridine, and inosine phosphates) in addition to adenine nucleotides were hydrolyzed. From analyses of the products of hydrolysis using HPLC, it was revealed that the monomeric chaperonin successively hydrolyzed the phosphoanhydride and phosphoester bonds of ATP in the order of *γ* to α. This activity was strongly suppressed by point mutation of specific essential aspartic acid residues. Although these archaeal monomeric chaperonins did not alter the refolding of MDH, their novel versatile nucleotide hydrolysis activity might fulfill a new function. Western blot experiments demonstrated that the monomeric chaperonin subunits were also present in lysed cell extracts of *T. acidophilum*, and partially purified native monomer displayed Co^{2+}-dependent AMPase activity.

Chaperonins, one of the most well studied molecular chaperones, assist in protein folding and inhibit protein aggregation both *in vivo* and *in vitro* (*1*, *2*). Based on sequence and structural similarities, chaperonins are classified into two groups: group I chaperonins found in bacteria, mitochondria, and chloroplasts and group II chaperonins found in eukaryotic cytosol and archaea (*2*, *3*). Among group I chaperonins, GroEL from *Escherichia coli*, in concert with its cochaperonin GroES, has been studied very thoroughly. The oligomeric complex of GroEL is composed of 14 identical 57-kDa subunits arranged in heptameric rings stacked back to back (*4*) and associates with a dome-shaping heptameric ring of 10-kDa GroES (*5*) to form a large central cavity, which proves a protective environment for proper folding of proteins. It undergoes ATP-induced conformational changes that are crucial for its folding function (*6*−*9*). In comparison, group II chaperonins form toroidal double rings with 8- or 9-fold rotary symmetry and function without a cofactor such as GroES, but the helical protrusion at the tip of the apical domain substitutes for the cofactor as a built-in lid for the central cavity (*3*). The eukaryotic group II chaperonin, TCP-1 ring complex (TRiC, also called CCT),[1] forms a hexadecameric complex composed of eight different subunits (*3*, *10*). Several eukaryotic proteins, such as actin and tubulin, may only be folded *in vitro* in the presence of CCT and Mg-ATP (*11*−*13*). Recent studies suggest that CCT interacts with polyglutamine-expanded variants of huntingtin (*14*, *15*), VHL tumor suppressor (*16*), and the G*β* WD40 proteins (*17*) and effectively inhibits their aggregation.

The group II chaperonin from *Thermoplasma acidophilum* (Ta-cpn) is composed of two stacked eight-membered rings of alternating α- and *β*-subunits (*18*) whose amino acid sequences are approximately 60% identical (*19*, *20*). Various studies using cryo-EM provided low-resolution images of group II chaperonins in a variety of conformations (*21*−*24*). A difference in secondary structure of the helical protrusion of apical domain between α- and *β*-subunits was also reported in both crystal structure studies (*25*) and NMR studies (*26*). The recombinant α-subunit from *T. acidophilum* forms a hexadecameric oligomer that binds adenine nucleotides tightly and possesses a low ATP hydrolysis activity (*27*). Recently, Hirai et al. (*28*) also reported that this recombinant α oligomer displayed not only ATPase activity but also GTPase, CTPase, UTPase activities in the presence of Mg^{2+}, Co^{2+}, and Mn^{2+} and also a corresponding chaperonin activity. The hydrolytic activity was confined to the nucleoside triphosphate, in contrast to a previous finding (*29*) that reported Co^{2+}- or Mn^{2+}-dependent ADP hydrolysis activities. Very recently, the group II chaperonin from *Pyrococcus furiosus* was also shown to have ATPase activity in the presence of Mg^{2+}, Co^{2+}, and Mn^{2+} ion (*30*).

In this study, we report that monomeric recombinant α-subunits (Ta-cpn α_1) and *β*-subunits (Ta-cpn β_1) from *T. acidophilum* display a novel nucleotide hydrolysis activity. We found that both Ta-cpn α_1 and Ta-cpn β_1 were capable of

†This work was partly supported by grants-in-aid for Scientific Research from the Ministry of Education, Culture, Sports, Science, and Technology of Japan, the Takeda Science Foundation, and a grant from the Venture Business Laboratory of Tottori University.

*Corresponding author. Tel: +81-857-31-5271. Fax: +81-857-31-5271. E-mail: kawata@bio.tottori-u.ac.jp.

[1]Abbreviations: CD, circular dichroism; CCT, chaperonin containing t-complex polypeptide; Gdn-HCl, guanidine hydrochloride; MDH, malate dehydrogenase; BSA, bovine serum albumin; Ta-cpn α_1, recombinant chaperonin α-monomers from *Thermoplasma acidophilum*; Ta-cpn β_1, recombinant chaperonin *β*-monomers from *T. acidophilum*; Ta-cpn α_{api}, apical domain of *T. acidophilum* α-subunit; Ta-cpn β_{api}, apical domain of *T. acidophilum* *β*-subunit.

Published on Web 09/03/2009

hydrolyzing various nucleoside triphosphates, diphosphates, and monophosphates in the presence of divalent metals (Mg^{2+}, Co^{2+}, and Mn^{2+}). The nucleotides were hydrolyzed successively from γ-phosphate to α-phosphate. Ta-cpn monomers with this AMPase activity were detected in the cell lysates of *T. acidophilum*, suggesting that the monomeric form of this chaperonin and its corresponding nucleotide hydrolysis activity may be biologically relevant. Our present results hint at a new functional role of archaeal group II chaperonin proteins.

EXPERIMENTAL PROCEDURES

Cloning and Plasmids. The structural genes (*T. acidophilum* Ta0980 and Ta1276) of *T. acidophilum* chaperonin α-subunit and β-subunit were amplified from genomic DNA by PCR (*19*) and inserted into pET23a(+) vector (Novagen) to produce pET-Ta-cpnα and pET-Ta-cpnβ. Alanine substitution mutants of chaperonins were generated by site-directed mutagenesis of these plasmids using the QuikChange kit (Stratagene). The amplified gene and chaperonin mutants were confirmed by DNA sequence analysis.

Expression and Protein Purification. For expression of Ta-cpn α, Ta-cpn β, and mutant proteins, *E. coli* BL21(DE3) was transformed with the constructed plasmid, and transformants were grown at 37 °C in LB medium in the presence of 50 μg/mL ampicillin overnight. For purification of all proteins, harvested cells were resuspended in 50 mM Hepes−KOH, pH 7.4, containing 2 mM EDTA, 1 mM DTT, and 1 mg/mL Pefabloc, lysed by sonication on ice, and centrifuged. The supernatants were heated at 55 °C for 30 min and cooled immediately on ice. Heat-aggregated proteins were removed by centrifugation and filtration. Soluble proteins were then loaded onto a Resource-Q anion-exchange column (GE Healthcare), which had been equilibrated with 50 mM Hepes−KOH, pH 7.4, containing 2 mM EDTA and 1 mM DTT, and eluted with a 0−600 mM KCl linear gradient using an ÄKTA-FPLC system at 4 °C. Fractions containing Ta-cpn α, Ta-cpn β, and mutant proteins were pooled and concentrated using Amicon-10 (M_w 10000 cutoff filter). The preparations were loaded onto a Superdex 200-10/300GL column (GE Healthcare) equilibrated with 50 mM Hepes−KOH, pH 7.4, containing 150 mM KCl. Hexadecameric chaperonins were eluted immediately after the void volume, and monomeric chaperonins were eluted later. Fractions containing monomeric chaperonin were heated at 55 °C for 30 min in 50 mM Hepes−KOH, pH 7.0, containing 10 mM KCl, 5 mM $MgCl_2$, and 4 mM ATP and cooled immediately on ice. After centrifugation, the supernatants were incubated at 4 °C for 30 min in 50 mM Hepes−KOH, pH 7.0, containing 10 mM EDTA. This sample was dialyzed against 50 mM Hepes−KOH, pH 7.4, containing 150 mM KCl at 4 °C. The purity of the purified proteins was checked by 15% SDS−PAGE, and the proteins were identified by analysis of the N-terminal amino acid sequence on a SHIMADZU PPSQ-10 protein sequencer. Protein concentrations of purified proteins were determined by using the commercial protein assay kit (Bio-Rad) with BSA as a standard.

CD Spectra Measurement. Far-UV CD spectra were recorded at 190−250 nm with a Jasco J-720 spectropolarimeter equipped with a constant temperature cell holder at 25 °C. Sixteen independent scans were accumulated and recorded using a 1 mm light path length cell to obtain the display spectra. Protein concentrations were 0.05 mg/mL in 5 mM Tris-HCl, pH 7.4.

Nucleotide Hydrolysis Activity Assay. Various nucleotides of the highest grade were purchased from Wako (Osaka) and Sigma. Nucleotide hydrolysis activity was measured routinely as follows. Reaction mixtures containing 4.8 μM Ta-cpn α_1 or Ta-cpn β_1 in reaction buffer (50 mM Hepes−KOH, pH 7.0, containing 10 mM KCl and one of the following chloride salts: 5 mM $MgCl_2$, 2 mM $CoCl_2$, or 5 mM $MnCl_2$) were incubated for 10 min at 55 °C. In experiments to determine the optimal temperature of ATPase activity, the reaction buffer containing monomeric chaperonin was incubated for 10 min at various temperatures. Reaction was started by addition of 4 mM nucleotide. The reaction was stopped by addition of 7% perchloric acid, and then the quantity of inorganic phosphate (P_i) produced during the reaction was determined colorimetrically with the malachite green reagent (*31*). All assays were performed at least in triplicate, and data are displayed as averages ± standard error.

Activity staining of chaperonin in PAGE gels was performed as follows. Nondenaturing gels containing monomeric chaperonins were incubated in 50 mM Hepes−KOH buffer, pH 7.0, containing 10 mM KCl, 4 mM nucleotides, and either 5 mM $MgCl_2$, 2 mM $CoCl_2$, or 5 mM $MnCl_2$ for 90 min at 55 °C. After incubation, the gels were quickly rinsed with water. Inorganic phosphate (P_i) produced in the native gels was determined colorimetrically with the malachite green reagent as described (*32*).

HPLC Analysis of Nucleotides. HPLC analysis of nucleotide was performed as follows. Reaction mixtures containing 4.8 μM Ta-cpn α_1 or Ta-cpn β_1 or 25 μM Ta-cpn α_1 or Ta-cpn β_1 in reaction buffer (50 mM Hepes−KOH, pH 7.0, containing 10 mM KCl and 2 mM $CoCl_2$) were incubated for 10 min at 55 °C. Reaction was started by addition of 2 mM nucleotide. Five μL of reaction mixture was applied to a Mono-Q HR5/5 anion-exchange column (Amersham Biosciences) and was analyzed using a Gilson-UniPoint HPLC system at 25 °C at a flow rate of 1 mL/min, with a linear NH_4HCO_3 gradient (10−600 mM). Nucleotides were detected using absorbance at 260 nm (*33*). Quantitation of nucleotides was performed by calculation of the peak area of each nucleotide. The total area of all nucleotide peaks at time 0 was used as a reference (100%).

Chaperonin Activity (*Protein Refolding*) *Assay*. The chaperonin activity of Ta-cpn α_1 or Ta-cpn β_1 was measured by using *Thermus* sp. MDH (M_w 35000 × dimer) as described by Hirai et al. (*28*). *Thermus* sp. MDH was purchased from Amano Enzyme Inc. (Nagoya, Japan).

Thermostability of MDH in the presence of monomeric chaperonins was determined by adding 0.026 μM native *Thermus* sp. MDH into buffer (50 mM Hepes−KOH, pH 7.0, containing 10 mM KCl) containing 0.17 μM monomeric chaperonin at 50 °C. At appropriate intervals, MDH activity was determined.

Cultivation of T. acidophilum Cells and Western Blot Analysis. *T. acidophilum* cells stored in 8% glycerol (3 mL) at −80 °C were used to inoculate 50 mL of medium containing 0.1% yeast extract, 60 mM dextrose, 20 mM KH_2PO_4, 2 mM $MgSO_4$, 50 mM $(NH_4)_2SO_4$, and 1.7 mM $CaCl_2 \cdot 2H_2O$ (aerobic condition medium (*34*)). The pH was adjusted to 1.65 with H_2SO_4. The cells were grown at 59 °C on a rotary shaker rotated at 90 rpm until the optical density at OD_{600} reached 0.4. Then, 10 mL of culture was transferred to 300 mL of the medium and then cultivated for 1 week at 59 °C under identical aeration conditions. The cells were harvested by centrifugation at 4000*g* for 15 min at 4 °C. The harvested cells were osmotically disrupted by suspension into 50 mM Hepes−KOH buffer, pH 7.0, containing 1 mg/mL

Pefabloc (*35*). The lysate was centrifuged at 100000*g* for 30 min at 4 °C. The supernatant was loaded onto Superdex 200-10/300GL gel-filtration column (GE Healthcare) equilibrated with 50 mM Hepes−KOH, pH 7.4, containing 150 mM KCl. The fractionated preparations were resolved by 10% SDS−PAGE, transferred to PVDF membranes, and stained using antibodies for Ta-cpn α or Ta-cpn β.

Preparation of Antibody. The apical domain fragments of Ta-cpn α (Ta-cpn α_{api}) and Ta-cpn β (Ta-cpn β_{api}) were obtained as follows. First, the gene regions of the apical domains of Ta-cpn α and Ta-cpn β were PCR-amplified and inserted into pET23a-(+) vector (Novagen). This insertion adds a His tag at the C-terminus of each fragment. *E. coli* BL21(DE3) was transformed with the constructed plasmids and was grown at 37 °C in LB medium in the presence of 50 μg/mL ampicillin overnight. Harvested cells were resuspended in 50 mM Hepes−KOH, pH 7.4, containing 150 mM KCl, lysed by sonication on ice, and centrifuged. Soluble proteins were then loaded onto a metal affinity resin (Clontech) column equilibrated with 50 mM Tris-HCl, pH 8.0, containing 150 mM NaCl, and eluted with a 0−300 mM imidazole linear gradient at room temperature. Fractions containing Ta-cpn α_{api} and Ta-cpn β_{api} were pooled and concentrated using Amicon-10 (M_w 10000 cutoff filter). The preparations were incubated at 25 °C for 30 min in 50 mM Hepes−KOH, pH 7.0, containing 10 mM EDTA. Ta-cpn α_{api} and Ta-cpn β_{api} were dialyzed with 50 mM Hepes−KOH, pH 7.4, containing 150 mM KCl at 4 °C. Finally, the preparations were loaded onto a Superdex 200-10/300GL column (GE Healthcare) equilibrated with 50 mM Hepes−KOH, pH 7.4, containing 150 mM KCl in order to obtain purified protein. Preparation of rabbit polyclonal antibodies for Ta-cpn α and Ta-cpn β was performed by Scrum (Tokyo) using the purified Ta-cpn α_{api} and Ta-cpn β_{api}, respectively. Immunoprecipitation experiments of chaperonins in *T. acidophilum* cell extracts were performed using the Seize X protein A immunoprecipitation kit (Pierce).

RESULTS

Structural Characteristics of Ta-cpn α and Ta-cpn β. In a previous study, we performed the structural and functional characterization of a hexadecameric chaperonin composed exclusively of Ta-cpn α from *T. acidophilum* (*28*). In that study, we noticed that there were lower molecular mass species in purified Ta-cpn α preparations that corresponded to the monomeric subunit form. In the present study, we attempted to investigate further the characteristics of these low molecular mass species of recombinant Ta-cpn α and Ta-cpn β, which we were able to isolate only as monomers in the previous study. We initially examined the quaternary structure using gel-filtration column chromatography. As shown in Figure 1A, the apparent molecular mass of monomeric Ta-cpn α and Ta-cpn β samples corresponded to that of hexadecameric Ta-cpn α (Ta-cpn α_{16}) denatured in 5 M urea, suggesting that these species are monomeric Ta-cpn α (Ta-cpn α_1) and β (Ta-cpn β_1). The purity of each chaperonin sample was confirmed by SDS−PAGE (Figure 1B). A 2 h incubation at 55 °C in the presence of ATP and either Mg^{2+}, Co^{2+}, or Mn^{2+} ion failed to convert either sample into higher oligomers. Co-ADP and Co-AMP were similarly ineffective.

Next, the secondary structure of Ta-cpn α_1 and Ta-cpn β_1 was examined by measuring the CD spectra, as shown in Figure 1C. Both Ta-cpn α_1 and Ta-cpn β_1 displayed similar secondary structures. Notably, the CD spectrum of Ta-cpn α_1 was almost identical to that of Ta-cpn α_{16} (*28*), suggesting that Ta-cpn α_1,

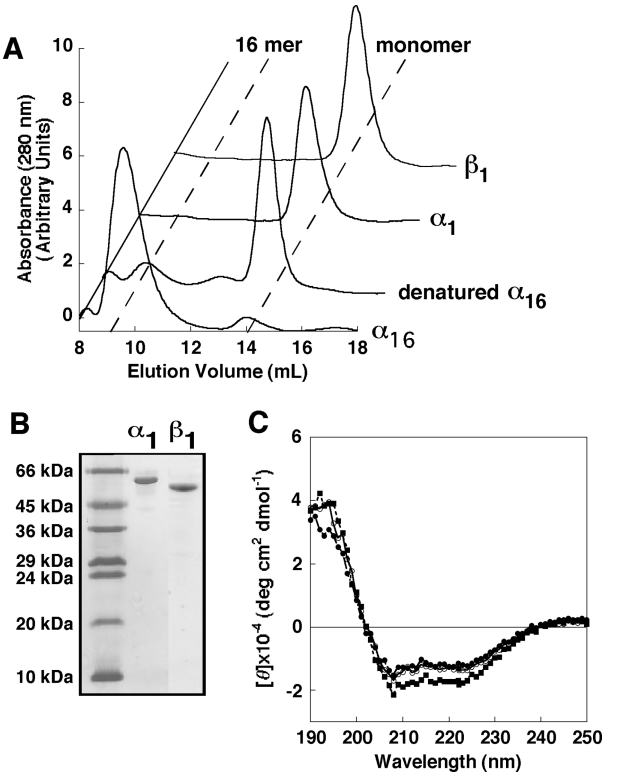

FIGURE 1: Structural characteristics of purified Ta-cpn α_1 and Ta-cpn β_1. (A) Oligomeric structure determined on a Superdex 200-10/300 GL column. The elution profiles of the purified Ta-cpn α_1 and Ta-cpn β_1 resulted in a profile that was identical to Ta-cpn α_{16} denatured in 5 M urea. (B) SDS−PAGE (15% polyacryamide gel) of the purified Ta-cpn α_1 and Ta-cpn β_1. (C) Far-UV CD spectra of Ta-cpn α_1 (closed circles), Ta-cpn β_1 (closed squares), and Ta-cpn α_{16} (open circles) in 5 mM Tris-HCl buffer, pH 7.4 at 25 °C. The protein concentrations were 50 μg/mL.

and by association, Ta-cpn β_1, may assume secondary structures very similar to that found in native $\alpha_8\beta_8$ *T. acidophilum* chaperonin (*20*). These findings prompted us to examine the functional characteristics of Ta-cpn α_1 and Ta-cpn β_1 in more detail.

ATPase Activity. The basis of function in chaperonins is the ATP-driven reaction cycle, in which substrate proteins are assisted to fold and the ATP bound to chaperonin is hydrolyzed. Previously, we reported that Ta-cpn α_{16} displayed NTPase activities in the presence of Mg^{2+} ion at 60 °C (*28*). Furthermore, Ta-cpn α_{16} also exhibited a weak ATPase activity in the presence of Co^{2+} or Mn^{2+} ion. We therefore studied the nucleotide hydrolysis activities of Ta-cpn α_1 and Ta-cpn β_1 under various conditions.

Interestingly, as shown in Figure 2A, Ta-cpn α_1 hydrolyzed ATP in the presence of Co^{2+}, Mn^{2+}, or Mg^{2+} ion. This ATPase activity was suppressed thoroughly upon addition of 10 mM EDTA, indicating the specific effects of these metal ions. The ATPase activity in the presence of Co^{2+} ion was the highest, a result that was in contrast to that for Ta-cpn α_{16}. As shown in Figure 2B, Ta-cpn β_1 also showed a similar ATPase activity in the presence of Co^{2+} ion, and a weak ATPase activity was observed in the presence of Mn^{2+} or Mg^{2+} ion. The activities were also suppressed by addition of EDTA. The optimal temperature for the ATPase activities of Ta-cpn α_1 and Ta-cpn β_1 in the presence of Co^{2+}, Mn^{2+}, or Mg^{2+} ion was around 55 °C (Figure 2C,D), which is almost the same as the optimal growth temperature of *T. acidophilum*. It should be noted that these Ta-cpn α_1 and β_1 chaperonins remained in the monomeric state under these

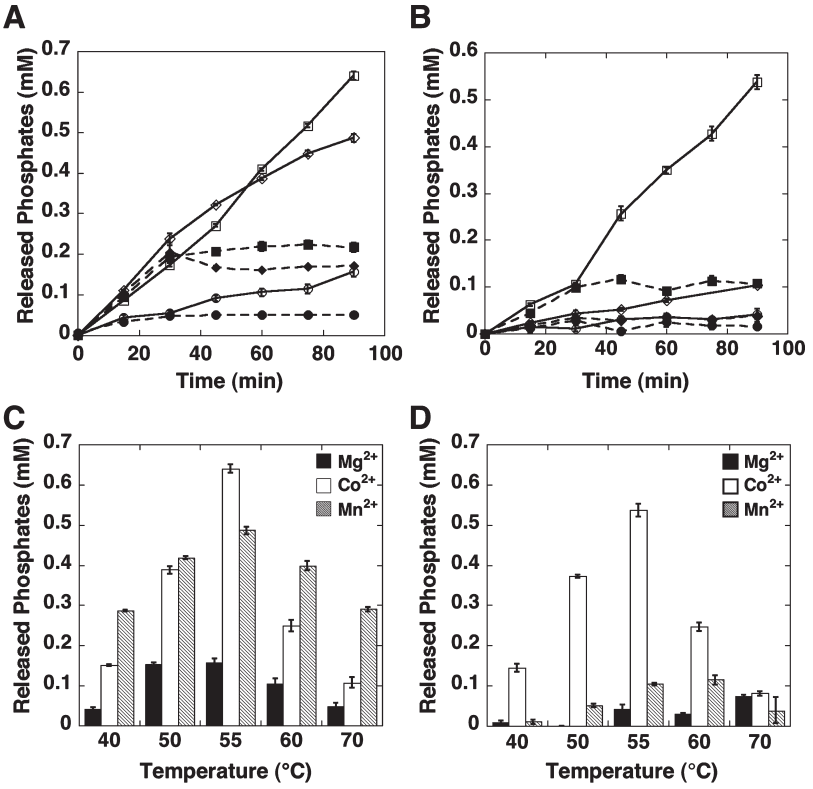

FIGURE 2: ATP hydrolysis activity of the monomeric chaperonins. Metal-dependent ATPase activity of (A) Ta-cpn α_1 and (B) Ta-cpn β_1 in the presence of Mg^{2+} (circles), Co^{2+} (squares), and Mn^{2+} (diamonds). Ten millimolar EDTA was added into the reaction mixture at 15 min (broken lines). ATPase activity of (C) Ta-cpn α_1 and (D) Ta-cpn β_1 in the presence of 5 mM Mg^{2+}, 2 mM Co^{2+}, or 5 mM Mn^{2+} at different temperatures. Released P_i was measured using the malachite green reagent after 90 min incubation at the indicated temperature. The concentrations of Ta-cpn α_1 and Ta-cpn β_1 were 4.8 μM.

conditions, since no higher oligomeric species were observed by gel-filtration analysis under the ATPase assay conditions. This was confirmed by performing activity staining of Ta-cpn α_1 and Ta-cpn β_1 in nondenaturing gel in the presence of Mg^{2+}, Co^{2+}, or Mn^{2+} ion, as shown in Figure 3. The activity staining of *E. coli* GroEL (14-mer) in the presence of Mg^{2+} ion is shown as a control in Figure 3A, i.e., where it may be seen that ATP was hydrolyzed but ADP and AMP were not. The ATP hydrolysis activities of Ta-cpn α_1 and Ta-cpn β_1 (at monomeric position in the gel) in the presence of Mg^{2+}, Co^{2+}, or Mn^{2+} ion are shown in panels B and C of Figure 3, respectively. The ATP hydrolysis activity of Ta-cpn β_1 in the presence of either Mg^{2+} or Mn^{2+} ion was very low compared to the activity of Ta-cpn α_1. Although we could not analyze the activities quantitatively, the results obtained using activity staining agreed with the results in Figure 2C, D. This indicated that the ATP hydrolysis (P_i-releasing) activities of these two chaperonin samples were derived from monomeric chaperonin.

Other Nucleotide Hydrolysis Activities. We next examined if Ta-cpn α_1 and Ta-cpn β_1 could hydrolyze nucleotides other than ATP, because we previously found that some archaeal chaperonins possess ADP-dependent functional activity (*29*). As shown in Figure 4A, Ta-cpn α_1 displayed an ability to hydrolyze ADP in the presence of Co^{2+}, Mn^{2+}, or Mg^{2+} ion at 55 °C. Very surprisingly, Ta-cpn α_1 also displayed an AMPase activity in the presence of these metal ions. Ta-cpn β_1 also showed ADPase and AMPase activities in the presence of Co^{2+} ion, whereas almost no hydrolysis of these nucleotides was observed in the presence of Mn^{2+} or Mg^{2+} (Figure 4B). Again, using activity staining of gels, we confirmed that these nucleotide hydrolysis activities were derived from monomeric chaperonin forms (Figures 3B,C).

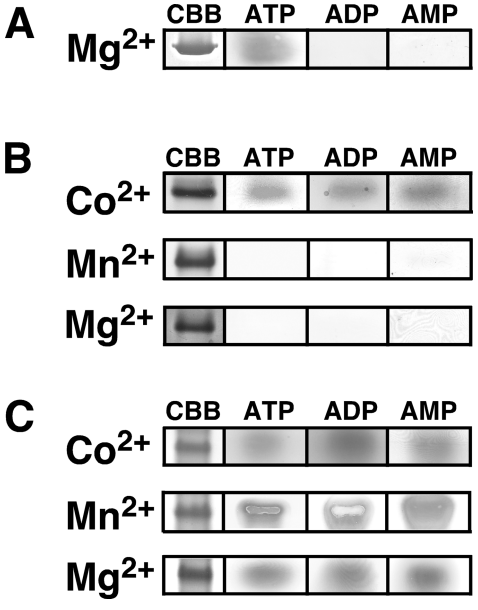

FIGURE 3: Nondenaturing gels stained for nucleotide hydrolysis activity. ATP, ADP, and AMP hydrolysis activities of (A) GroEL in the presence of 5 mM Mg^{2+} ion, (B) Ta-cpn β_1, and (C) Ta-cpn α_1 in the presence of 2 mM Co^{2+}, 5 mM Mn^{2+}, or 5 mM Mg^{2+} ion at 55 °C. CBB indicates the proteins in native gel by Coomassie Brilliant Blue staining.

Activity staining in the presence of ADP or AMP resulted in similar outcomes, which suggested that the nucleotide hydrolysis activities were derived from monomeric chaperonins. With regard to the Co-AMPase activities of Ta-cpn α_1 and Ta-cpn β_1, we determined that the K_m for AMP of these two chaperonins

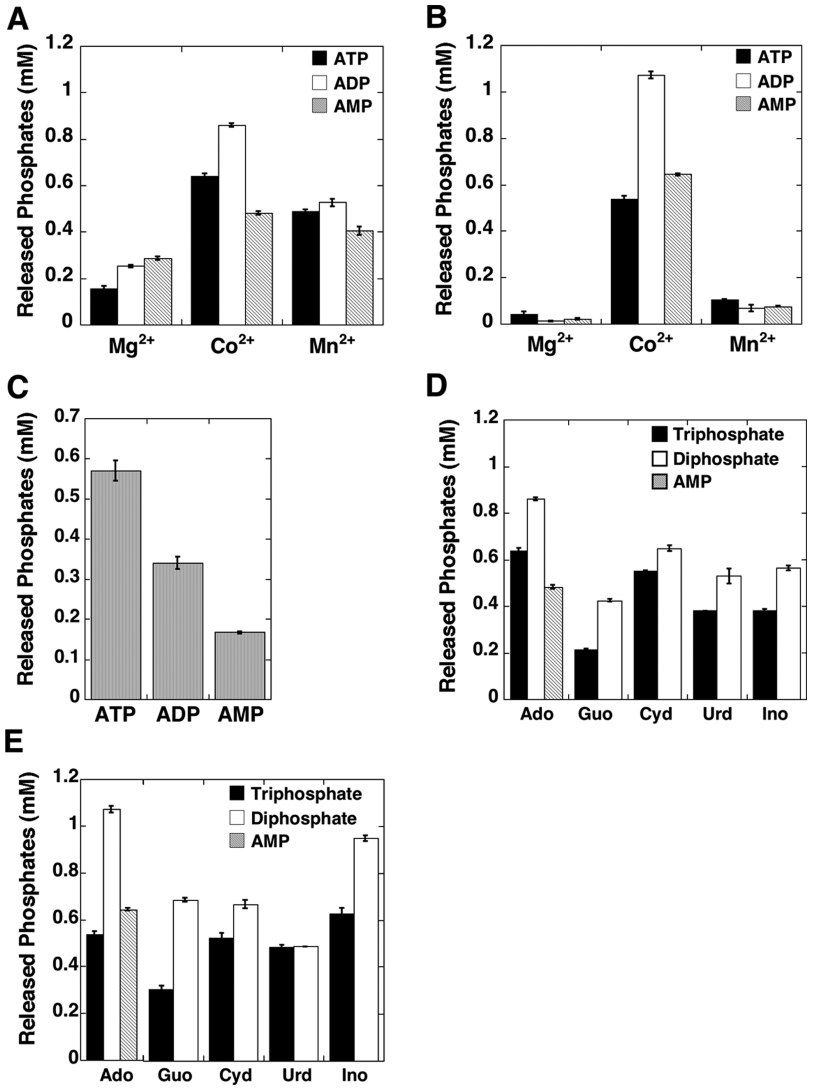

FIGURE 4: ATP, ADP, and AMP hydrolysis activities of the monomeric chaperonins. ATP, ADP, and AMP hydrolysis activities of (A) Ta-cpn α_1 and (B) Ta-cpn β_1 in the presence of 5 mM Mg^{2+}, 2 mM Co^{2+}, or 5 mM Mn^{2+} at 55 °C. (C) Exhaustive hydrolysis of 0.2 mM ATP, ADP, and AMP by Ta-cpn β_1 in the presence of 2 mM Co^{2+} ion at 55 °C for 90 min. Under these conditions, all nucleotides were hydrolyzed completely. A small amount of released P_i attributed to spontaneous degradation in the absence of chaperonin was subtracted from the raw data. Nucleotide hydrolysis assays of (D) Ta-cpn α_1 and (E) Ta-cpn β_1 in the presence of 2 mM Co^{2+} at 55 °C. Abbreviations: Ado (adenosine), Guo (guanosine), Cyd (cytidine), Urd (uridine), and Ino (inosine). The concentrations of Ta-cpn α_1 and Ta-cpn β_1 were 4.8 μM.

were less than 50 μM (data not shown). Further characterization was not possible at this point due to experimental limitations (the availability of radioactive AMP). This novel AMP hydrolysis activity shown by Ta-cpn α_1 and Ta-cpn β_1 is the first example of its kind, not only with regard to chaperonins but also with regard to archaeal enzymes in general. We compared the apparent rates of P_i release from ATP, ADP, and AMP of Ta-cpn α_{16}, Ta-cpn α_1, and Ta-cpn β_1 in the presence of Mg^{2+}, Co^{2+}, or Mg^{2+} ion. The results are summarized in Table 1.

In order to obtain an insight to the mechanism behind this novel hydrolysis activity, we hydrolyzed ATP, ADP, and AMP exhaustively with Ta-cpn β_1. As shown in Figure 4C, the ratio of the released inorganic phosphate concentrations observed from ATP, ADP, and AMP was about 3:2:1. This result suggested that the products of nucleotide hydrolysis consisted solely of orthophosphate. It was possible that Ta-cpn β_1 sequentially hydrolyzed nucleoside polyphosphates.

Next, we performed further assays using other nucleotides in the presence of Co^{2+} ion at 55 °C. As shown in Figure 4D,E, both chaperonins were able to hydrolyze various nucleoside triphosphates (GTP, CTP, UTP, and ITP) and diphosphates (GDP, CDP, UDP, and IDP). We could not examine the hydrolysis of nucleoside monophosphates, because commercial sources of these nucleotides were either unavailable or of insufficient purity. These results demonstrated that Ta-cpn α_1 and Ta-cpn β_1 were capable of hydrolyzing all of these types of nucleoside phosphate.

Next, in order to confirm that this novel nucleotide hydrolysis activity is in fact due to the monomeric chaperonin subunits and not to various contaminants, we constructed mutants of Ta-cpn α and Ta-cpn β. The amino acid residues subjected to mutation were aspartic acid residues (D67 or D394 for Ta-cpn α_1 and D62 or D391 for Ta-cpn β_1) that are regarded as active site residues of ATP hydrolysis (*20*, *36*). In the case of GroEL, it is well-known that mutation of the corresponding Asp398 to Ala results in a drastic decrease in ATP hydrolysis activity (*37*). Thus, four mutants, Ta-cpn α_1 D67A, Ta-cpn α_1 D394A, Ta-cpn β_1 D62A, and Ta-cpn β_1 D391A, were constructed, expressed, and purified in essentially the same manner as the wild-type proteins, and the structures of the purified mutants were similar to those of wild type (data not shown). We examined the ability to hydrolyze

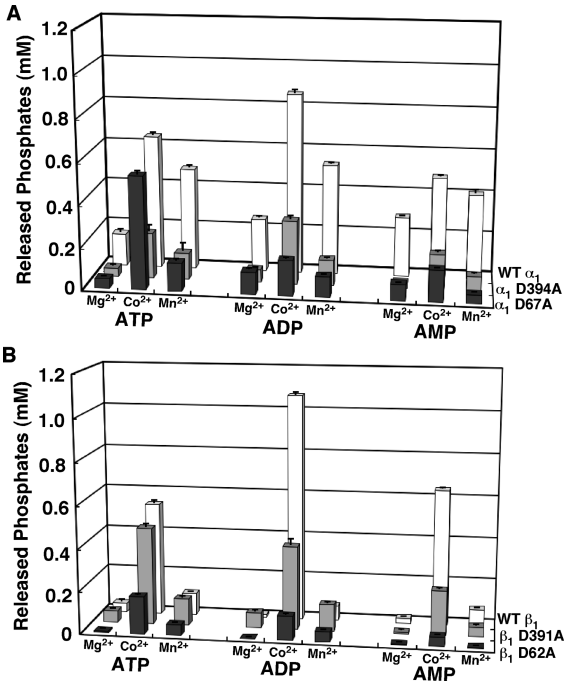

FIGURE 5: ATP, ADP, and AMP hydrolysis activities of wild-type monomeric chaperonin and mutants. (A) Comparison of Ta-cpn α_1 wild type, Ta-cpn α_1 D394A, and Ta-cpn α_1 D67A and (B) comparison of Ta-cpn β_1 wild type, Ta-cpn β_1 D391A, and Ta-cpn β_1 D62A in the presence of 5 mM Mg^{2+}, 2 mM Co^{2+}, or 5 mM Mn^{2+} at 55 °C after incubation for 90 min.

Table 1: Comparison of Nucleotide Hydrolysis Activities of Ta-cpn α_{16}, Ta-cpn α_1, and Ta-cpn β_1 in Terms of P_i Releasing Rate

		k_{app} (mol of P_i released·(mol of subunit^{-1})·min^{-1})		
nucleotide	metal	Ta-cpn α_{16} (at 60 °C)[a]	Ta-cpn α_1 (at 55 °C)	Ta-cpn β_1 (at 55 °C)
ATP	5 mM Mg^{2+}	0.28 ± 0.01	0.36 ± 0.03	0.10 ± 0.03
	2 mM Co^{2+}	0.17 ± 0.01	1.48 ± 0.02	1.24 ± 0.04
	5 mM Mn^{2+}	0.14 ± 0.01	1.13 ± 0.02	0.24 ± 0.01
ADP	5 mM Mg^{2+}	nd[b]	0.58 ± 0.01	0.03 ± 0.01
	2 mM Co^{2+}	nd	1.99 ± 0.01	2.48 ± 0.03
	5 mM Mn^{2+}	nd	1.22 ± 0.04	0.16 ± 0.03
AMP	5 mM Mg^{2+}	nd	0.66 ± 0.01	0.05 ± 0.01
	2 mM Co^{2+}	nd	1.12 ± 0.02	1.49 ± 0.01
	5 mM Mn^{2+}	nd	0.94 ± 0.04	0.18 ± 0.01

[a]Data taken from Hirai et al. (*28*). [b]nd: not detected.

ATP, ADP, and AMP for each of these mutants in the presence of Co^{2+}, Mn^{2+}, or Mg^{2+} ion at 55 °C. Panels A and B of Figure 5 show the results regarding Ta-cpn α_1 and Ta-cpn β_1, respectively. The ATP, ADP, and AMP hydrolysis activities of all of the mutants decreased significantly compared to wild type, with the notable exception of the ATP hydrolysis activities of Ta-cpn α_1 D67A and Ta-cpn β_1 D391A in the presence of Co^{2+} ion. In Ta-cpn α_1, Asp394 rather than Asp67 seemed to be more important to Co^{2+}-dependent ATPase activity, whereas in Ta-cpn β_1, Asp62 rather than Asp391 seemed to be more important. That such a difference exists in the contribution of individual Asp residues to ATP hydrolysis activity between Ta-cpn α_1 and Ta-cpn β_1 suggested that there may be minute differences in the active site structures of α- and β-subunits. These mutants of Ta-cpn α_1 and Ta-cpn β_1 also displayed a significantly decreased hydrolysis activity toward other nucleoside phosphates, such as guanosine, cytidine, uridine, and inosine phosphates (data not shown). From these results, we may conclude that monomers of *T. acidophilum* chaperonin subunit α and β possess a novel metal-dependent nucleoside phosphate(s) hydrolysis activity.

HPLC Analysis of Nucleotide Hydrolysis. In order further to understand how Ta-cpn α_1 and Ta-cpn β_1 hydrolyze nucleoside phosphate(s), we performed semiquantitative analyses of nucleotide hydrolysis using HPLC (*29*, *33*). Typical results for the hydrolytic activity of Ta-cpn α_1, starting from either ATP, ADP, or AMP in the presence of Co^{2+} ion at 55 °C, are shown in panels A, B, and C of Figure 6, respectively. As shown in the analyses (right panel in Figure 6A), ATP decreased in the presence of Ta-cpn α_1 gradually, concomitant with a slight increase in ADP and adenosine. A very small amount of AMP was detected (see left panel). For ADP, the gradual decrease in ADP was accompanied by an increase in mainly adenosine. Interestingly, the amount of AMP did not increase at all during the reaction (Figure 6B). Here, it should be noted that the sums of the area of all nucleotide peaks that appeared at any time were almost the same as the peak area of the initial ATP, ADP, or AMP at time 0 (right panels in Figure 6), suggesting that there were no missing or no undetectable nucleotides during the reaction. The hydrolysis rates as detected by decrease of ATP, ADP, and AMP determined from these data were 5.2 ± 0.2, 5.9 ± 0.8, and 8.5 ± 1.6 μM/min, respectively. The rate of AMP hydrolysis was greatest, which would account for the observation that the amount of AMP detected during the hydrolysis reactions was low. We also obtained similar results when we used Ta-cpn β_1 under the same conditions (data not shown). The hydrolysis rates of Ta-cpn β_1 for ATP, ADP, and AMP were 3.8 ± 1.0, 6.0 ± 0.9, and 6.7 ± 0.3 μM/min, respectively. These results demonstrated clearly that ATP, ADP, and AMP were hydrolyzed to produce adenosine by Ta-cpn α_1 and Ta-cpn β_1. Furthermore, we also confirmed that guanosine, cytidine, uridine, and inosine could be detected from the corresponding hydrolysis reactions by Ta-cpn α_1 and Ta-cpn β_1 (data not shown), indicating that these monomeric chaperonins can hydrolyze various nucleotides to their corresponding nucleosides.

To exclude the possibility that adenylate kinase (which catalyzes 2ADP ⇔ ATP + AMP) (*38*) from *E. coli* is contaminating our preparations, we performed these HPLC assays in the presence of a specific inhibitor for adenylate kinase, P^1,P^5-di(adenosyl-5′-)-pentaphosphate (*39*). Even in the presence of a molar excess (7.2 mM) of the inhibitor in the assay buffer, similar HPLC analysis patterns in ATP, ADP, and AMP hydrolysis activity assays were observed (data not shown), demonstrating that contribution of adenylate kinase activities was negligible.

Next, to understand the nucleotide hydrolysis mechanism in more detail, we examined whether the monomer chaperonins are able to hydrolyze ATP-γS or ADP-βS under the same conditions. If the monomer chaperonins are able to hydrolyze the phosphate bonds of β and α positions of the nucleoside triphosphate directly (i.e., endo-type hydrolysis), ATP-γS and ADP-βS would be hydrolyzed to AMP and adenosine, respectively. If the chaperonins can only hydrolyze phosphate from the external position (i.e., exo-type hydrolysis), ATP-γS and ADP-βS should not be hydrolyzed. As shown in Figure 7, both Ta-cpn α_1 and Ta-cpn β_1 were unable to hydrolyze ATP-γS and ADP-βS, as no significant amounts of AMP or adenosine were detected in the HPLC analyses. This result indicated that Ta-cpn α_1 and Ta-cpn β_1 may hydrolyze ATP and ADP to adenosine successively from the

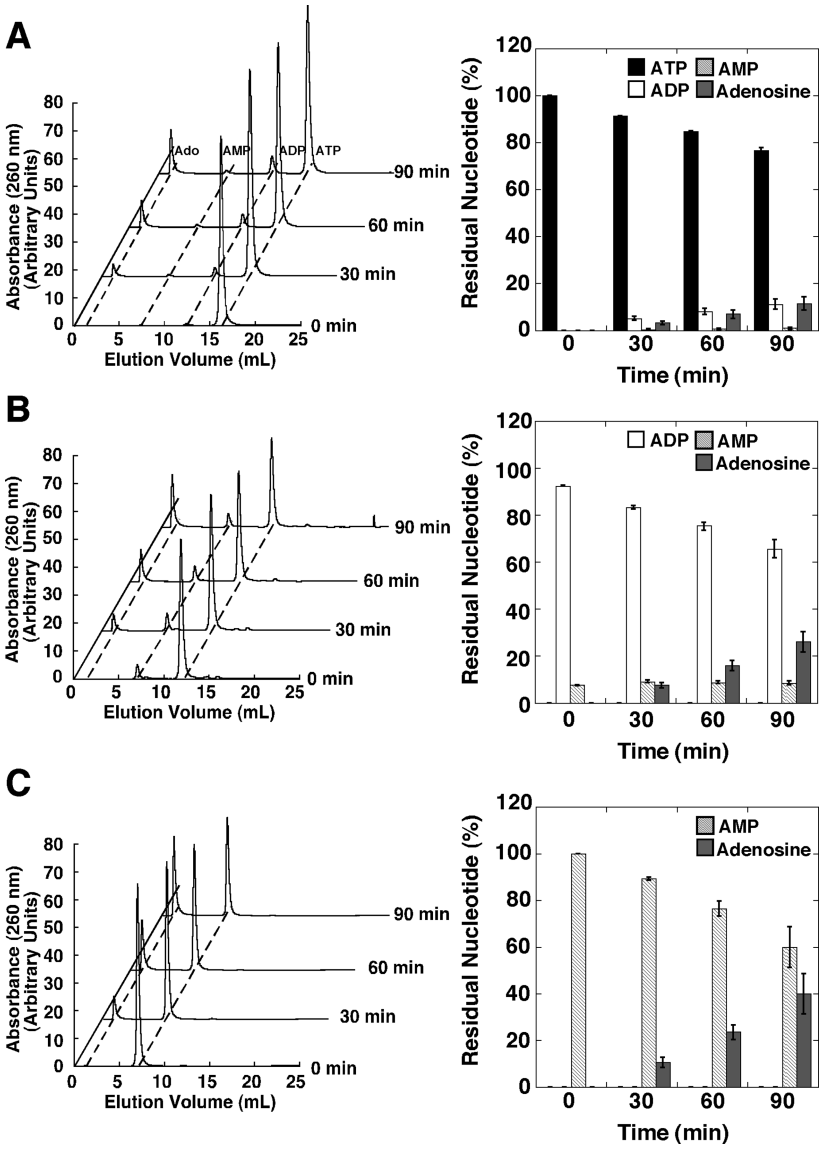

FIGURE 6: Identification of nucleotide intermediates during ATP, ADP, and AMP hydrolysis reactions. The reactions were performed by 4.8 μM Ta-cpn α_1 in the presence of 2 mM Co^{2+} at 55 °C, using the HPLC system described in the Experimental Procedures section. Right panels indicate the elution profiles of (A) ATP, (B) ADP, and (C) AMP hydrolysis reactions after incubation for 0, 30, 60, and 90 min, and left panels indicate the relative peak areas of each nucleotide observed over the time course of each reaction. The total peak area of each nucleotide at 0 time was set to 100%.

external γ and β positions, respectively, to the α position, i.e., ATP → ADP + P_i → AMP + 2P_i → adenosine + 3P_i. This was also supported by the fact that when we hydrolyzed ATP, ADP, and AMP with Ta-cpn β_1 exhaustively, the relative concentration of the inorganic phosphate released from ATP, ADP, and AMP corresponded to ratios of 3:2:1 (Figure 4C).

Chaperonin Activity of Ta-cpn α_1 and Ta-cpn β_1. Next, we examined the chaperonin activities of Ta-cpn α_1 and Ta-cpn β_1, i.e., whether *T. acidophilum* monomeric chaperonin subunits were able to assist protein folding or to protect a substrate protein from thermal aggregation. We used *Thermus* sp. MDH as a substrate protein, since refolding of this protein was assisted by Ta-cpn α_{16} in a previous study (*28*). Even in the presence of excess Ta-cpn α_1 or Ta-cpn β_1 without nucleotides, the refolding of MDH from 6 M Gdn-HCl at 50 °C was not arrested and proceeded to 60−70% yield within 5 min, and this refolding yield was retained over the next 25 min. The relative stability of refolded MDH in the presence of chaperonins, relative to the spontaneous reaction, seemed to be due to nonspecific interactions between substrate protein and the chaperonin protein. This was confirmed by experiments in the presence of BSA (data not shown).

The thermal stability of MDH at 50 °C was enhanced in the presence of excess Ta-cpn α_1 or Ta-cpn β_1; i.e., almost 100% of the initial activity of MDH was retained over 60 min (data not shown). Since a gradual decrease to 80% in 60 min of MDH activity was observed in the presence of BSA, Ta-cpn α_1 and Ta-cpn β_1 may have some specific protective effects toward MDH thermal denaturation. This effect was observed regardless of the presence or absence of divalent cations and nucleotides. These results indicated that although Ta-cpn α_1 and Ta-cpn β_1 do not actively assist protein folding, they may passively protect a protein from thermal unfolding.

Identification of the Chaperonin Subunits in T. acidophilum Cells. In order to clarify that the Ta-cpn α_1 and Ta-cpn β_1 forms characterized in this study are not merely artifactual monomeric chaperonin subunits expressed and purified from *E. coli*, we attempted to detect the existence of monomeric

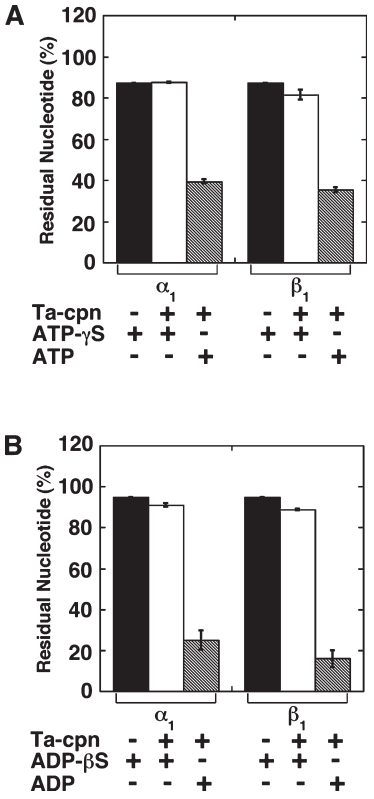

FIGURE 7: Hydrolysis activity of nucleotide analogues. (A) ATP-γS and (B) ADP-βS hydrolysis activities of Ta-cpn α_1 (25 μM) and Ta-cpn β_1 (25 μM) in the presence of 2 mM Co^{2+} at 55 °C after incubation for 90 min. Nucleotides were quantified by the HPLC analysis system described in Figure 5.

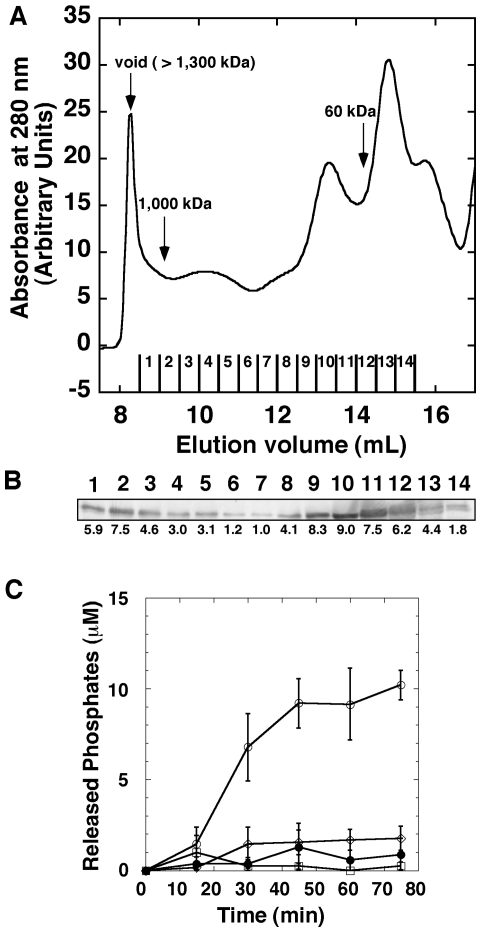

FIGURE 8: Identification of monomeric chaperonins in freshly prepared lysates of *T. acidophilum* cells using gel-filtration column chromatography. (A) Chromatogram from the Superdex 200-10/300GL column. (B) Typical Western blot analysis with an antibody for Ta-cpn α_{api}. Numeric values under the bands represent the relative concentration of the monomeric chaperonins when fraction 7 was set as 1.0. (C) AMP hydrolysis activity assay of the fraction sample corresponding to monomeric chaperonin (fractions 9−12). Key: circles, low molecular fraction of *T. acidophilum* cell lysate; squares, bovine serum albumin; diamonds, green fluorescent protein; closed circles, cell lysate supernatants subjected to immunoprecipitation against an antibody for Ta-cpn α_{api}. The protein concentrations in the assay were all 1 mg/mL.

chaperonins in archaeal *T. acidophilum* cells. As shown in Figure 8A,B, freshly prepared cell extracts from *T. acidophilum* cells were immediately subjected to gel-filtration column chromatography, followed by Western blot analysis using Ta-cpn α_{api} or Ta-cpn β_{api} antibodies. Since we used polyclonal antibodies in this experiment, we could not detect α- and β-subunit separately; i.e., a very similar Western blotting pattern was observed for both antibodies. However, as shown in Figure 8B, the result showed that both high (above 1000 kDa) and low (about 60 kDa) molecular mass species, which presumably correspond to the fully assembled and the monomeric chaperonins, respectively, were present even in the archaeal *T. acidophilum* cell extracts.

Next, we performed the AMP hydrolysis activity assay of the lower molecular mass fractions in order to clarify if the species from *T. acidophilum* cells with smaller molecular mass were functionally similar to those we characterized above. As shown in Figure 8C, the low molecular mass species also displayed an AMP hydrolysis activity in the presence of Co^{2+} ion at 55 °C, although other protein samples, such as bovine serum albumin or green fluorescent protein did not display any AMP hydrolysis activity. Most interestingly, when the supernatant of *T. acidophilum* cell lysate was subjected to immunoprecipitation against the anti-chaperonin antibodies, this AMPase activity was depleted. This finding demonstrated that, in addition to fully assembled chaperonin, monomeric chaperonin subunits also exist in archaeal *T. acidophilum* cells and exhibit this novel nucleotide hydrolysis activity.

DISCUSSION

The functional aspects of archaeal group II chaperonin are still unclear, because the function and structure of archaeal chaperonin are different depending on the origins. Here, we studied the chaperonin from archaeal bacterium *T. acidophilum* as a model for group II chaperonin structure/function. From the expression pattern of the α and β chaperonins from *T. acidophilum* in *E. coli*, we found that a fraction of these chaperonins existed as structured subunits (Figure 1). These monomeric chaperonins, Ta-cpn α_1 and Ta-cpn β_1, were found to exhibit a metal (Mg^{2+}, Co^{2+}, Mn^{2+}) dependent ATPase activity (Figure 2). Furthermore, this activity was extended to ADP and AMP as well, especially in the presence of Co^{2+} ion (Figures 3, 4, and 5 and Table 1). The corresponding guanosine, cytidine, uridine, and inosine phosphates were also hydrolyzed (Figure 4). The hydrolysis of ATP was found to proceed according to a successive mechanism: ATP → ADP → AMP → adenosine, according to our experiments. Mutation of two distinct aspartic acid residues demonstrated that this successive hydrolytic mechanism was supported by these aspartic residues (Figures 4, 5, 6, and 7). Although Ta-cpn α_1 and Ta-cpn β_1 did not show any active participation in the refolding reaction of MDH, they showed a slight protective effect with regard to thermal inactivation. Finally, we showed that native

monomeric chaperonins also existed in *T. acidophilum* cells and that these chaperonins displayed AMPase activity (Figure 8). This is, to our knowledge, the first demonstration of an archaeal monomeric chaperonin that displays such a broad nucleotide hydrolysis activity, especially including a novel AMPase activity, in the presence of Co^{2+} ion.

Nucleotide Hydrolysis Activity of the Structured Monomeric Chaperonin α and β. It is well-known that the ATP hydrolysis activity in both group I and group II chaperonins is important during facilitation of the refolding of nonnative substrate proteins and folding of newly synthesized polypeptide, by coordinating the conformational changes of individual domains in the oligomer (*37*, *40*−*42*). With regard to the group I chaperonins, a single chaperonin subunit usually could not work as an ATPase on its own. However, a monomeric GroEL variant has been shown to bind ATP (*43*), and a truncated GroEL monomer (*44*) and a monomeric *Thermus thermophilus* chaperonin variant (*45*) have been shown to possess an ability to promote folding of a substrate protein. Chaperonins from *Mycobacterium tuberculosis*, which exist as lower order oligomers due to weak subunit interactions, were also reported to possess a very weak Mg-ATPase activity and the ability to suppress aggregation of a substrate protein (*46*). Very recently, it is also reported that monomeric archaeal chaperonin from *Methanocaldococcus jannaschii* possessed Mg-ATP hydrolysis activity and could protect a substrate protein against unfolding (*47*).

In the present study, α and β chaperonins from the archaea *T. acidophilum* were purified in structured monomeric form, and it was confirmed that the monomeric chaperonins showed very novel nucleotide hydrolysis activities that include ADPase and AMPase in the presence of divalent cations, notably Co^{2+} ion. In a previous study, we revealed that the oligomeric Ta-cpn α_{16} could only hydrolyze ATP, and not ADP or AMP, in the presence of Mg^{2+}, Co^{2+}, or Mn^{2+} ion (*28*). This difference in the nucleotide specificity between Ta-cpn α_1 and Ta-cpn α_{16} was interesting when we consider the hydrolysis mechanism. Only the monomeric form of the two chaperonins possessed ADPase and AMPase activities. Our previous results (*29*) that showed that recombinant α and β chaperonins from *T. acidophilum* showed ADPase activity may be attributed to the copurification of this monomeric chaperonin form with chaperonin oligomers.

We identified two aspartic acid residues (Asp394 and Asp67) that were very important for the ATPase activities of both the monomeric and oligomeric forms of Ta-cpn α (Figure 5 and data not shown). From the X-ray crystallographic studies of native $\alpha_8\beta_8$ chaperonin from *T. acidophilum* (*20*, *36*), both Asp394 and Asp67 of the α-subunit are located in the vicinity of the γ-phosphate group of ATP and form hydrogen bonds with this phosphate through a water molecule. The hydrogen-bonded water molecule was presumably activated during ATP hydrolysis. Although we do not know the specifics of the active site structure of the monomeric chaperonin, a structure with a considerably high flexibility in this site, possibly caused by dissociation to monomers, may be formed. This high flexibility at the active site may allow the catalytic Asp residues to react with the β- and α-phosphates of nucleotides.

An interesting finding of the present study was the ability of chaperonin monomers to hydrolyze nucleoside monophosphate, i.e., NMPase activity in addition to nucleoside diphosphate in the presence of Co^{2+} ion. In archaea, some enzymes have been found that display an ADP hydrolysis activity. For example, phosphofructokinase and glucokinase from *P. furiosus* (*48*, *49*) and *Thermococcus* sp. (*50*) and DNA ligase from *Aeropyrum pernix* K1 (*51*) were shown to have ADP-dependent activities. In eukaryotic cells, nucleoside triphosphate diphosphohydrolase (NTPDase) in plasma membrane was shown to exert hydrolysis of extracellular ATP and ADP to AMP in the presence of divalent cations (usually Ca^{2+} or Mg^{2+} ion) (*52*). However, an enzyme with the ability to hydrolyze AMP has been reported only for 5′-nucleotidase (ecto-AMPase), which is involved in lymphocyte catabolism, converting extracellular AMP to adenosine (*53*). Thus, although some eukaryotic and archaea enzymes have been known to possess ADP and AMP hydrolysis activities, this is the first demonstration that monomeric α and β chaperonins from an archaeal source are capable of hydrolyzing multiple types of nucleoside phosphates.

A Possible Significance for Monomeric Chaperonin in Vivo. As shown in Figure 8, *T. acidophilum* cell extracts contained both oligomeric chaperonin and dissociated monomeric α- and β-subunit chaperonins. In our *in vitro* experiments, we did not observe the association of monomeric chaperonins into higher oligomers under the conditions we tested and, as such, could not perform detailed experiments regarding the relationship between the nucleotide hydrolysis activities of chaperonin oligomer versus monomer and the significance of this relationship *in vivo*. However, in this context, it was very interesting to note that the monomeric chaperonins were present even in *T. acidophilum* cells. It has been reported that considerable dissociation of mammalian CCT to smaller oligomeric structures and free subunits may occur in the cell, even under physiological conditions (*54*). In agreement with this report, we also found in separate experiments that a large amount of CCT from bovine testis was localized as dissociated monomers during purifications (unpublished data). Together with these facts, it may be said that the group II chaperonins may regularly exist in monomeric form as well as the oligomeric form in their respective cells. Although we could not detect any changes in α- and β-subunit quantities under different cultivation conditions, such as a different cultivation temperature or the presence of various concentrations of metals, it is also interesting to note that changes in the subunit expression level of chaperonin from *Thermococcus* strain KS-1 may be controlled by cultivation temperature (*55*). A dynamic equilibrium of higher and lower oligomeric forms, with variations in the ratio of subunit components under different conditions, may also contribute an essential component of the function and mechanism of these proteins, as also seen in the case of small heat shock proteins (*56*, *57*).

When we consider a specific role for the dissociated monomeric chaperonin in *T. acidophilum* cells, one possible role of them is to protect proteins against thermal unfolding, although they are incapable of assisting the refolding of proteins. Protein folding and refolding would be performed by the native oligomeric chaperonin. A similar result that identified an aggregation suppression activity of proteins was also reported for a dissociated chaperonin form isolated from *M. tuberculosis* (*46*).

Another interesting finding was that the nucleotide hydrolysis activity of monomeric α- and β-subunit chaperonins was strongly Co^{2+}-dependent. Although the actual concentration of Co^{2+} ion in the cells is unknown, a cultivation medium containing divalent metals such as Co^{2+}, Mn^{2+}, and Zn^{2+} is usually used in the cultivation of archaeal cells (*34*). It has been reported recently that a divalent metal cation (Mg^{2+} and Co^{2+} ions, etc.) transporter exists ubiquitously in bacteria and archaea (*58*, *59*). Therefore, Co^{2+} ion may also be a physiologically relevant

regulator in *T. acidophilum*. A possible role of the monomeric chaperonins that have the Co^{2+}-dependent nucleoside phosphate(s) hydrolysis activity might be to produce inorganic phosphates within the cell. The released phosphate ions may be used in the maintenance of steady conditions within the cells, such as pH. It is noteworthy that the pH of the culture medium of *T. acidophilum* is about 2 (*34*). Further detailed studies of archaeal group II chaperonin, including the real function of the monomeric chaperonins *in vivo*, should be performed in near future.

REFERENCES

1. Bukau, B., and Horwich, A. L. (1998) The Hsp70 and Hsp60 chaperone machines. *Cell 92*, 351–366.
2. Hartl, F. U., and Hayer-Hartl, M. (2002) Molecular chaperones in the cytosol: from nascent chain to folded protein. *Science 295*, 1852–1858.
3. Gutsche, I., Essen, L. O., and Baumeister, W. (1999) Group II chaperonins: new TRiC(k)s and turns of a protein folding machine. *J. Mol. Biol. 293*, 295–312.
4. Braig, K., Otwinowski, Z., Hegde, R., Boisvert, D. C., Joachimiak, A., Horwich, A. L., and Sigler, P. B. (1994) The crystal structure of the bacterial chaperonin GroEL at 2.8 Å. *Nature 371*, 578–586.
5. Hunt, J. F., Weaver, A. J., Landry, S. J., Gierasch, L., and Deisenhofer, J. (1996) The crystal structure of the GroES co-chaperonin at 2.8 Å resolution. *Nature 379*, 37–45.
6. Gething, M. J., and Sambrook, J. (1992) Protein folding in the cell. *Nature 355*, 33–45.
7. Ranson, N. A., Farr, G. W., Roseman, A. M., Gowen, B., Fenton, W. A., Horwich, A. L., and Saibil, H. R. (2001) ATP-bound states of GroEL captured by cryo-electron microscopy. *Cell 107*, 869–879.
8. Yifrach, O., and Horovitz, A. (2000) Coupling between protein folding and allostery in the GroE chaperonin system. *Proc. Natl. Acad. Sci. U.S.A. 97*, 1521–1524.
9. Taniguchi, M., Yoshimi, T., Hongo, K., Mizobata, T., and Kawata, Y. (2004) Stopped-flow fluorescence analysis of the conformational changes in the GroEL apical domain: relationships between movements in the apical domain and the quaternary structure of GroEL. *J. Biol. Chem. 279*, 16368–16376.
10. Kubota, H., Hynes, G., Carne, A., Ashworth, A., and Willison, K. (1994) Identification of six Tcp-1-related genes encoding divergent subunits of the TCP-1-containing chaperonin. *Curr. Biol. 4*, 89–99.
11. Frydman, J., Nimmesgern, E., Erdjument-Bromage, H., Wall, J. S., Tempst, P., and Hartl, F. U. (1992) Function in protein folding of TRiC, a cytosolic ring complex containing TCP-1 and structurally related subunits. *EMBO J. 11*, 4767–4778.
12. Gao, Y., Thomas, J. O., Chow, R. L., Lee, G. H., and Cowan, N. J. (1992) A cytoplasmic chaperonin that catalyzes beta-actin folding. *Cell 69*, 1043–1050.
13. Yaffe, M. B., Farr, G. W., Miklos, D., Horwich, A. L., Sternlicht, M. L., and Sternlicht, H. (1992) TCP1 complex is a molecular chaperone in tubulin biogenesis. *Nature 358*, 245–248.
14. Tam, S., Geller, R., Spiess, C., and Frydman, J. (2006) The chaperonin TRiC controls polyglutamine aggregation and toxicity through subunit-specific interactions. *Nat. Cell Biol. 8*, 1155–1162.
15. Kitamura, A., Kubota, H., Pack, C. G., Matsumoto, G., Hirayama, S., Takahashi, Y., Kimura, H., Kinjo, M., Morimoto, R. I., and Nagata, K. (2006) Cytosolic chaperonin prevents polyglutamine toxicity with altering the aggregation state. *Nat. Cell Biol. 8*, 1163–1170.
16. Spiess, C., Miller, E. J., McClellan, A. J., and Frydman, J. (2006) Identification of the TRiC/CCT substrate binding sites uncovers the function of subunit diversity in eukaryotic chaperonins. *Mol. Cell 24*, 25–37.
17. Kubota, S., Kubota, H., and Nagata, K. (2006) Cytosolic chaperonin protects folding intermediates of Gbeta from aggregation by recognizing hydrophobic beta-strands. *Proc. Natl. Acad. Sci. U.S.A. 103*, 8360–8365.
18. Nitsch, M., Klumpp, M., Lupas, A., and Baumeister, W. (1997) The thermosome: alternating alpha and beta-subunits within the chaperonin of the archaeon *Thermoplasma acidophilum*. *J. Mol. Biol. 267*, 142–149.
19. Ruepp, A., Graml, W., Santos-Martinez, M. L., Koretke, K. K., Volker, C., Mewes, H. W., Frishman, D., Stocker, S., Lupas, A. N., and Baumeister, W. (2000) The genome sequence of the thermoacidophilic scavenger *Thermoplasma acidophilum*. *Nature 407*, 508–513.
20. Ditzel, L., Lowe, J., Stock, D., Stetter, K. O., Huber, H., Huber, R., and Steinbacher, S. (1998) Crystal structure of the thermosome, the archaeal chaperonin and homolog of CCT. *Cell 93*, 125–138.
21. Llorca, O., Smyth, M. G., Carrascosa, J. L., Willison, K. R., Radermacher, M., Steinbacher, S., and Valpuesta, J. M. (1999) 3D reconstruction of the ATP-bound form of CCT reveals the asymmetric folding conformation of a type II chaperonin. *Nat. Struct. Biol. 6*, 639–642.
22. Llorca, O., McCormack, E. A., Hynes, G., Grantham, J., Cordell, J., Carrascosa, J. L., Willison, K. R., Fernandez, J. J., and Valpuesta, J. M. (1999) Eukaryotic type II chaperonin CCT interacts with actin through specific subunits. *Nature 402*, 693–696.
23. Schoehn, G., Quaite-Randall, E., Jimenez, J. L., Joachimiak, A., and Saibil, H. R. (2000) Three conformations of an archaeal chaperonin, TF55 from *Sulfolobus shibatae*. *J. Mol. Biol. 296*, 813–819.
24. Schoehn, G., Hayes, M., Cliff, M., Clarke, A. R., and Saibil, H. R. (2000) Domain rotations between open, closed and bullet-shaped forms of the thermosome, an archaeal chaperonin. *J. Mol. Biol. 301*, 323–332.
25. Bosch, G., Baumeister, W., and Essen, L. O. (2000) Crystal structure of the beta-apical domain of the thermosome reveals structural plasticity in the protrusion region. *J. Mol. Biol. 301*, 19–25.
26. Heller, M., John, M., Coles, M., Bosch, G., Baumeister, W., and Kessler, H. (2004) NMR studies on the substrate-binding domains of the thermosome: structural plasticity in the protrusion region. *J. Mol. Biol. 336*, 717–729.
27. Gutsche, I., Mihalache, O., and Baumeister, W. (2000) ATPase cycle of an archaeal chaperonin. *J. Mol. Biol. 300*, 187–196.
28. Hirai, H., Noi, K., Hongo, K., Mizobata, T., and Kawata, Y. (2008) Functional characterization of the recombinant group II chaperonin {alpha} from *Thermoplasma acidophilum*. *J. Biochem. 143*, 505–515.
29. Hongo, K., Hirai, H., Uemura, C., Ono, S., Tsunemi, J., Higurashi, T., Mizobata, T., and Kawata, Y. (2006) A novel ATP/ADP hydrolysis activity of hyperthermostable group II chaperonin in the presence of cobalt or manganese ion. *FEBS Lett. 580*, 34–40.
30. Luo, H., Laksanalamai, P., and Robb, F. T. (2009) An exceptionally stable Group II chaperonin from the hyperthermophile *Pyrococcus furiosus*. *Arch. Biochem. Biophys. 486*, 12–18.
31. Lanzetta, P. A., Alvarez, L. J., Reinach, P. S., and Candia, O. A. (1979) An improved assay for nanomole amounts of inorganic phosphate. *Anal. Biochem. 100*, 95–97.
32. Zlotnick, G. W., and Gottlieb, M. (1986) A sensitive staining technique for the detection of phosphohydrolase activities after polyacrylamide gel electrophoresis. *Anal. Biochem. 153*, 121–125.
33. Horst, M., Oppliger, W., Feifel, B., Schatz, G., and Glick, B. S. (1996) The mitochondrial protein import motor: dissociation of mitochondrial hsp70 from its membrane anchor requires ATP binding rather than ATP hydrolysis. *Protein Sci. 5*, 759–767.
34. Robb, F. T., Place, A. R., Sowers, K. R., Schreier, H. J., DasSarma, S., and Fleischmann, E. M. (1995) Archaea: a laboratory manual , Cold Spring Harbor Laboratory Press, Cold Spring Harbor, NY.
35. Searcy, D. G. (1976) *Thermoplasma acidophilum*: intracellular pH and potassium concentration. *Biochim. Biophys. Acta 451*, 278–286.
36. Steinbacher, S., and Ditzel, L. (2001) Nucleotide binding to the thermoplasma thermosome: implications for the functional cycle of group II chaperonins. *J. Struct. Biol. 135*, 147–156.
37. Rye, H. S., Burston, S. G., Fenton, W. A., Beechem, J. M., Xu, Z., Sigler, P. B., and Horwich, A. L. (1997) Distinct actions of cis and trans ATP within the double ring of the chaperonin GroEL. *Nature 388*, 792–798.
38. Schulz, G. E., Schiltz, E., Tomasselli, A. G., Frank, R., Brune, M., Wittinghofer, A., and Schirmer, R. H. (1986) Structural relationships in the adenylate kinase family. *Eur. J. Biochem. 161*, 127–132.
39. Schulz, G. E., Muller, C. W., and Diederichs, K. (1990) Induced-fit movements in adenylate kinases. *J. Mol. Biol. 213*, 627–630.
40. Yoshida, T., Yohda, M., Iida, T., Maruyama, T., Taguchi, H., Yazaki, K., Ohta, T., Odaka, M., Endo, I., and Kagawa, Y. (1997) Structural and functional characterization of homo-oligomeric complexes of alpha and beta chaperonin subunits from the hyperthermophilic archaeum *Thermococcus* strain KS-1. *J. Mol. Biol. 273*, 635–645.
41. Weissman, J. S., Rye, H. S., Fenton, W. A., Beechem, J. M., and Horwich, A. L. (1996) Characterization of the active intermediate of a GroEL-GroES-mediated protein folding reaction. *Cell 84*, 481–490.
42. Guagliardi, A., Cerchia, L., and Rossi, M. (1995) Prevention of in vitro protein thermal aggregation by the *Sulfolobus solfataricus* chaperonin. Evidence for nonequivalent binding surfaces on the chaperonin molecule. *J. Biol. Chem. 270*, 28126–28132.

43. White, Z. W., Fisher, K. E., and Eisenstein, E. (1995) A monomeric variant of GroEL binds nucleotides but is inactive as a molecular chaperone. *J. Biol. Chem. 270*, 20404–20409.
44. Makino, Y., Taguchi, H., and Yoshida, M. (1993) Truncated GroEL monomer has the ability to promote folding of rhodanese without GroES and ATP. *FEBS Lett. 336*, 363–367.
45. Taguchi, H., Makino, Y., and Yoshida, M. (1994) Monomeric chaperonin-60 and its 50-kDa fragment possess the ability to interact with non-native proteins, to suppress aggregation, and to promote protein folding. *J. Biol. Chem. 269*, 8529–8534.
46. Qamra, R., Srinivas, V., and Mande, S. C. (2004) *Mycobacterium tuberculosis* GroEL homologues unusually exist as lower oligomers and retain the ability to suppress aggregation of substrate proteins. *J. Mol. Biol. 342*, 605–617.
47. Bergeron, L. M., Lee, C., Tokatlian, T., Hollrigl, V., and Clark, D. S. (2008) Chaperone function in organic co-solvents: Experimental characterization and modeling of a hyperthermophilic chaperone subunit from *Methanocaldococcus jannaschii*. *Biochim. Biophys. Acta 1784*, 368–378.
48. Kengen, S. W., Tuininga, J. E., de Bok, F. A., Stams, A. J., and de Vos, W. M. (1995) Purification and characterization of a novel ADP-dependent glucokinase from the hyperthermophilic archaeon *Pyrococcus furiosus*. *J. Biol. Chem. 270*, 30453–30457.
49. Tuininga, J. E., Verhees, C. H., van der Oost, J., Kengen, S. W., Stams, A. J., and de Vos, W. M. (1999) Molecular and biochemical characterization of the ADP-dependent phosphofructokinase from the hyperthermophilic archaeon *Pyrococcus furiosus*. *J. Biol. Chem. 274*, 21023–21028.
50. Selig, M., Xavier, K. B., Santos, H., and Schonheit, P. (1997) Comparative analysis of Embden-Meyerhof and Entner-Doudoroff glycolytic pathways in hyperthermophilic archaea and the bacterium *Thermotoga*. *Arch. Microbiol. 167*, 217–232.
51. Jeon, S. J., and Ishikawa, K. (2003) A novel ADP-dependent DNA ligase from *Aeropyrum pernix* K1. *FEBS Lett. 550*, 69–73.
52. Kaczmarek, E., Koziak, K., Sevigny, J., Siegel, J. B., Anrather, J., Beaudoin, A. R., Bach, F. H., and Robson, S. C. (1996) Identification and characterization of CD39/vascular ATP diphosphohydrolase. *J. Biol. Chem. 271*, 33116–33122.
53. Kaissling, B., Spiess, S., Rinne, B., and Le Hir, M. (1993) Effects of anemia on morphology of rat renal cortex. *Am. J. Physiol. 264*, F608–F617.
54. Roobol, A., Grantham, J., Whitaker, H. C., and Carden, M. J. (1999) Disassembly of the cytosolic chaperonin in mammalian cell extracts at intracellular levels of K^+ and ATP. *J. Biol. Chem. 274*, 19220–19227.
55. Yoshida, T., Ideno, A., Hiyamuta, S., Yohda, M., and Maruyama, T. (2001) Natural chaperonin of the hyperthermophilic archaeum, *Thermococcus* strain KS-1: a hetero-oligomeric chaperonin with variable subunit composition. *Mol. Microbiol. 39*, 1406–1413.
56. Haslbeck, M., Walke, S., Stromer, T., Ehrnsperger, M., White, H. E., Chen, S., Saibil, H. R., and Buchner, J. (1999) Hsp26: a temperature-regulated chaperone. *EMBO J. 18*, 6744–6751.
57. Sugino, C., Hirose, M., Tohda, H., Yoshinari, Y., Abe, T., Giga-Hama, Y., Iizuka, R., Shimizu, M., Kidokoro, S., Ishii, N., and Yohda, M. (2009) Characterization of a sHsp of *Schizosaccharomyces pombe*, SpHsp15.8, and the implication of its functional mechanism by comparison with another sHsp, SpHsp16.0. *Proteins 74*, 6–17.
58. Smith, R. L., and Maguire, M. E. (1995) Distribution of the CorA Mg^{2+} transport system in gram-negative bacteria. *J. Bacteriol. 177*, 1638–1640.
59. Eshaghi, S., Niegowski, D., Kohl, A., Martinez Molina, D., Lesley, S. A., and Nordlund, P. (2006) Crystal structure of a divalent metal ion transporter CorA at 2.9 angstrom resolution. *Science 313*, 354–357.